

# UPCommons

**Portal del coneixement obert de la UPC**

<http://upcommons.upc.edu/e-prints>

---

© 2017. Aquesta versió està disponible sota la llicència CC-BY-NC-ND 4.0 <http://creativecommons.org/licenses/by-nc-nd/4.0/>

© 2017. This version is made available under the CC-BY-NC-ND 4.0 license <http://creativecommons.org/licenses/by-nc-nd/4.0/>

---

# On the use of a dedicated ballast pellet for a prompt self-ejection mechanism after a temperature transient in lead-cooled fast reactors

Francisco J. Arias\*

*Department of Fluid Mechanics, University of Catalonia  
ESEIAAT C/ Colom 11, 08222 Barcelona, Spain*

---

## Abstract

The potential use of changes in buoyancy as a reactivity feedback mechanism during temperature transients in heavy liquid metal fast reactors (HLMFRs) is discussed. It is shown that with the use of ballast pellets ( $\sim 15\%$  volume fraction) introduced in combination with fuel pellets, fuel rods will be endowed with a reliable self-ejection mechanism that is able to compensate temperature transients. Utilizing a simplified model, an estimate of the negative reactivity insertion expected from this mechanism is derived. The use of ballast pellets opens up the possibility of introducing greater amounts of actinides into the core, as well as providing a solution to the classical problem of positive coolant temperature reactivity coefficients in fast reactors.

*Keywords:* Heavy liquid metal fast reactors, buoyancy, temperature transient compensation, Generation IV reactors

---

## 1. Introduction

One of the unique features of heavy liquid metal fast reactors (HLMFRs) with lead or lead-bismuth eutectic coolant is the very high density of the coolant: the coolant density in HLMFRs is similar to that of the fuel. The potential use of this feature has either been overlooked by nuclear designers or seen as a “nuisance”, and, as a result, preventive measures such as the

---

\*Corresponding author

*Email address:* francisco.javier.arias@upc.edu (Francisco J. Arias)

use of tungsten deadweight (ballast) to overcome buoyancy forces have been proposed [3, 7].

The objective of this study was to assess the potential for exploiting  
10 changes in buoyancy forces as a control mechanism for fuel rod self-ejection  
during HLMFR temperature transients, thereby providing a reliable solution  
to the well-established problem of the positive coolant temperature reactiv-  
ity coefficient exhibited by sodium fast reactors and also in lead-cooled fast  
reactors depending on the size of the reactor core. This concept is expected  
15 to represent a passive safety feature for the system but it does not represent  
at all a control device to be used during reactor normal operation.

The effect of buoyancy forces in HLMFRs as a positive aspect in safety  
analysis during a post-accident heat removal scenario was recently investi-  
gated by Arias [4]. It was found that, because of the similar densities of the  
20 fuel and the heavy liquid metal (HLM) coolant, an inherent passive safety  
feedback self-removal mechanism governed by buoyancy is developed, pro-  
pelling the packed bed away from the wall, and preventing temperatures  
that could jeopardize the structural integrity of the vessel being reached,  
as well as reducing the re-criticality potential by limiting the allowable bed  
25 depth.

Thus, it is interesting to consider whether buoyancy forces, rather than  
being regarded as a nuisance during nominal operating conditions, can be  
harnessed as a mechanism for endowing fuel rods with unique safety prop-  
erties only available in HLMFRs. In the sections that follow, this possibility  
30 will be investigated and discussed. However, the reader should be aware that  
the results reported in this preliminary analysis of the proposed concept are  
based on idealizations, of the sort which are inevitable in preliminary the-  
oretical assessments of concepts, and therefore should not be misconstrued  
as definitive detailed analysis. The final verdict about the feasibility of the  
35 proposed concept will only be reached following detailed analysis of the com-  
plexities arising from the proposed solutions, the subject of future work.  
Nonetheless, we feel that this preliminary assessment is appropriate at this  
time, to encourage (or not) further careful investigation of the idea.

## 2. Buoyancy forces as a fuel rod ejection mechanism

40 Fig. 1 illustrates schematically the mechanism we seek to exploit. For the  
envisaged mechanism to work as intended the density of the coolant needs

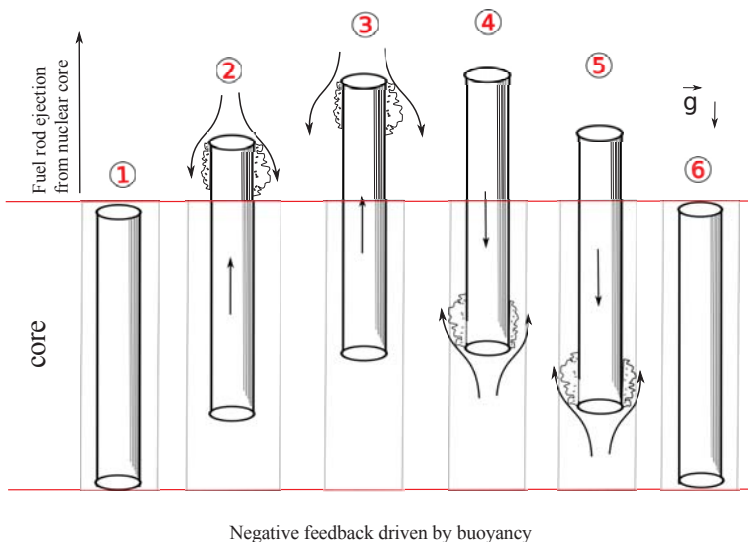


**Fig. 1.** Fuel rod ejection by buoyancy forces. Sequence: (1) Insertion of reactivity, leading to rising temperatures; (2) Due to relative changes in density with temperature, buoyancy effects act and the fuel rod is propelled upwards; (3) A subcriticality condition is reached, leading to falling temperatures; (4) Relative changes in density lead to loss of buoyancy and the fuel rod falls back down; (5) Fuel rod re-enters the core; (6) End of transient.

to become greater than the effective density of the fuel as the temperature increases.

Fig. 2 shows the variation of density as a function of temperature for mixed oxide (MOX) and  $\text{UO}_2$  fuels and Pb-Bi eutectic and Pb coolants. This indicates that the relative changes of HLM coolant and fuel densities with temperature are not favorable. However, before deciding on the feasibility of the posited buoyancy mechanism, the fuel densities shown in Fig. 2 need to be corrected to account for the presence of stainless steel, mostly in the form of cladding. Thus, to take into account the effect of stainless steel on the total density of the fuel, a combined fuel-steel density may be defined as:

$$\bar{\rho}_f = F_f \rho_f + (1 - F_f) \rho_s \quad (1)$$

where  $F_f$  is the volume fraction of fuel and  $\rho_f$  and  $\rho_s$  are the densities of the fuel and stainless steel, respectively.

For practical purposes, the densities can be approximated as linear functions of temperature:

$$\rho_i = \rho_{i,0} - \alpha_i T_i \quad (2)$$

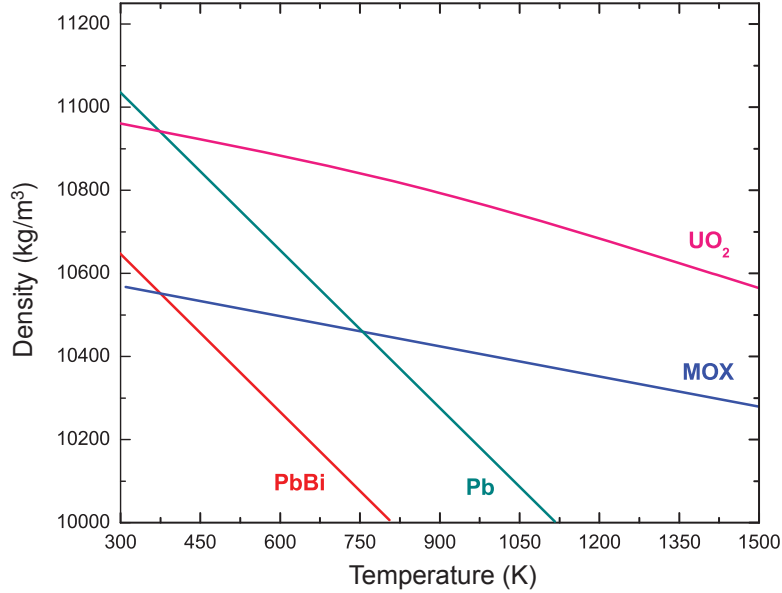


**Fig. 2.** Density variations of Pb-Bi eutectic and Pb coolants and MOX and UO<sub>2</sub> fuels as functions of temperature.

where the subscript  $i$  denotes the specific material, for example,  $i = f$  for fuel,  $c$  for coolant,  $s$  for stainless steel, and  $\rho_{i,0}$  is the density of material  $i$  at a temperature of 0 K,  $\alpha_i$  is the rate of change of density of material  $i$  with temperature, and  $T_i$  is the temperature of material  $i$  in K. Then, the combined density given by Eq. (1) can be represented as a function of temperatures as:

$$\bar{\rho}_f = \bar{\rho}_{f,0} - \bar{\alpha}_f T_f \quad (3)$$

where

$$\bar{\rho}_{f,0} = [F_f \rho_{f,0} + (1 - F_f) \rho_{s,0}] \quad (4)$$

and

$$\bar{\alpha}_f = (1 - F_f) \frac{T_s}{T_f} \alpha_s \quad (5)$$

where  $T_s$  is the average temperature of the cladding and can be calculated as  $T_s = T_f - \Delta T$ , with  $\Delta T$  being the temperature drop between fuel and cladding. A typical value of  $\Delta T$  is  $\sim 200$  K. This value has been assumed for the preliminary calculations in this paper.

From the available data in the literature, the linear relationships for fuels [17], coolants [16] and stainless steel [12] shown in Table 1 were formulated.

70 All densities are given in  $\text{kg m}^{-3}$  for temperatures in K. The corresponding relationships are depicted in Fig. 3, where a volume fraction of stainless steel of 45.6% (from Table 2) was assumed.

**Table 1.** Assumed density variations with temperature.

Material type	Material	Equation
Coolant	Pb	$\rho_{\text{Pb}} = 11478.69 - 1.32T_c$
Coolant	PbBi	$\rho_{\text{PbBi}} = 11093.71 - 1.33T_c$
Fuel	UO <sub>2</sub>	$\rho_{\text{UO}_2} = 11122.84 - 0.36T_f$
Fuel	MOX	$\rho_{\text{MOX}} = 10657.97 - 0.255T_f$
Cladding	Stainless steel SS-316	$\rho_s = 8077.729 - 0.42T_s$
Ballast	Tungsten	$\rho_w = 19300.0 - 0.22T_f$

Referring to Fig. 3, it can be seen the densities of the HLM coolants are consistently greater than those of the combined fuel-steel options. Thus, the desired buoyancy mechanism for self-ejection of a fuel rod will only be possible with the use of deadweight or ballast to increase the effective density of the fuel. The use of such ballast is discussed below.

### 2.1. The tungsten ballast pellet

Although the use of tungsten as ballast in lead-cooled reactors has been proposed previously, its application was for a totally different purpose: tungsten ballast is located outside the core and used to keep the fuel assemblies in their designated positions by providing a downward force exceeding the force due to buoyancy under refueling conditions [2]. In other words, buoyancy forces are not contemplated as the basis of a feedback mechanism but, rather, they are neutralized over all temperatures by the use of an excess of ballast.

The proposed use of tungsten ballast here is with a totally different purpose in mind. We want to neutralize buoyancy, but only in the nominal range of working temperatures of the reactor, and we want buoyancy forces to appear if the nominal operating temperature range is exceeded, for example during a temperature or power transient. So, by introducing a tungsten ballast pellet occupying just the right volume within the fuel rod (as depicted in Fig. 4) we will be able to endow the fuel rod with a reliable mechanism for self-ejection or self-disassembly, as depicted in Fig. 1.

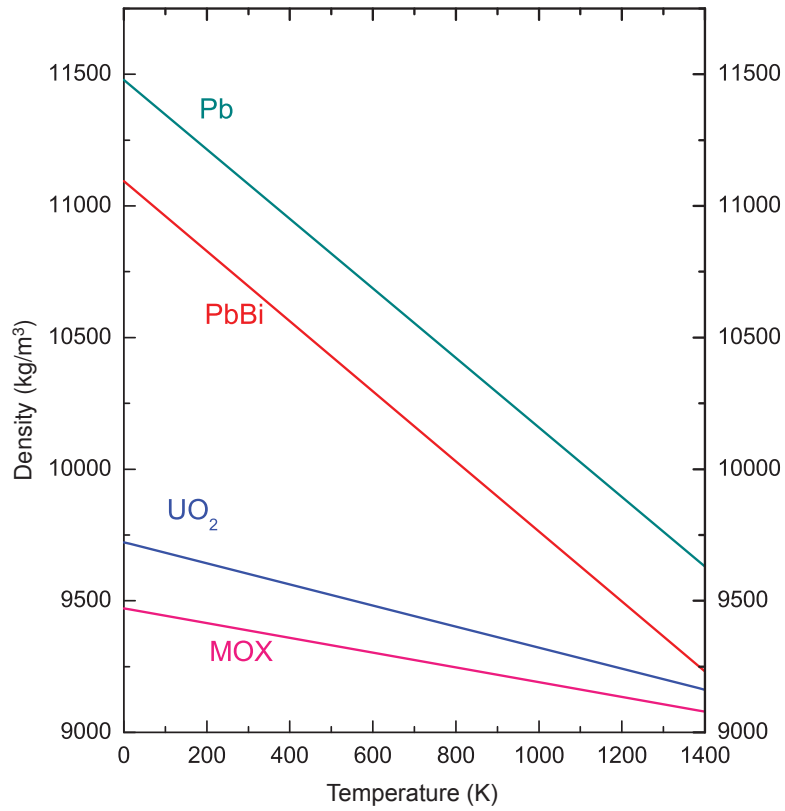


**Fig. 3.** Density variations as functions of temperature of Pb-Bi eutectic and Pb coolants and MOX- and UO<sub>2</sub>-based fuels with a representative volume of stainless steel cladding.

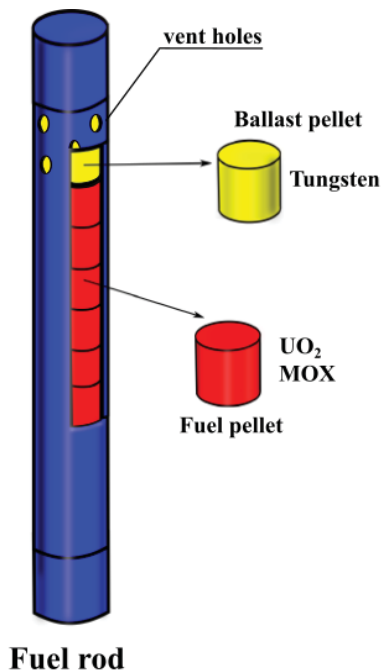


**Fig. 4.** The ballast pellet concept: by introducing a ballast pellet into the fuel rod it is possible to harness buoyancy forces to provide negative reactivity feedback.

95 Our first step, therefore, is to derive an expression that allows us to determine what tungsten ballast pellet fraction will be needed, and our second step is to establish an initial estimate of the negative reactivity insertion arising from the consequent fuel rod self-ejection.

100 First, we need to define an “effective density” taking into account the volume fraction occupied by tungsten ballast pellets. Proceeding as in our previous analysis, the effective fuel-steel-tungsten density is:

$$\rho_{f,\text{eff}} = (1 - F_b)\bar{\rho}_f + F_b\rho_w \quad (6)$$

where  $F_b$  is the volume fraction of tungsten ballast used and  $\rho_w$  its density. From our foregoing discussion, Eq. (6) yields the following relationship:

$$\rho_{\text{eff}} = \rho_{\text{eff},0} - \alpha_{\text{eff}}T_f \quad (7)$$

where

$$\rho_{\text{eff},0} = (1 - F_b)\bar{\rho}_{f,0} + F_b\rho_{w,0} \quad (8)$$

105 Design considerations dictate that the ballast pellet should be positioned at the top or bottom of the fuel element, thereby avoiding thermal stresses between fuel pellets, and also enabling the ballast pellet to act as a reflector (thanks to the high density of tungsten) and/or as a bottom- or top-cap, as schematically indicated in Fig. 4. The design of the ballast pellet will also

110 be influenced by the location of the gas plenum. If the gas plenum is at the same end of the fuel element as the ballast, then the ballast pellet should contain holes to allow the free flow of fission gas towards the plenum.

Thus, accounting for the contribution due to the expansion of the ballast, the effective rate of change of density is

$$\alpha_{\text{eff}} = (1 - F_b)\bar{\alpha}_f + F_b \frac{T_w}{T_f} \alpha_w \quad (9)$$

115 where  $T_w$  is the temperature of the ballast at the appropriate location. Because of the high thermal conductivity of tungsten ( $\kappa_w \approx 173 \text{ WK}^{-1}\text{m}^{-1}$ ),  $T_w$  can be assumed to be approximately equal to the local temperature of the fuel. The fuel temperature falls by around 50% between its maximum axial value (close to the center of the fuel element) and the outermost axial  
 120 levels where the ballast should be placed. Thus, to be on the safe side, a conservative preliminary value for the effective ballast temperature is taken as  $T_w \approx \frac{1}{2}T_f$ . In overestimating the temperature of tungsten, we are underestimating its density and thus overestimating the volume fraction needed. From the available literature [12], the density of tungsten fits the relationship  
 125 given in Table 1.

Fuel rod ejection driven by buoyancy will only occur when the effective density of the fuel becomes lower than that of the surrounding coolant, or:

$$\rho_c > \rho_{\text{eff}} \quad (10)$$

To progress our analysis, we need an expression connecting the temperature of the fuel with the temperature of the coolant at the same instant  
 130 in time. It should be noted, however, that even if the condition given by Eq. (10) is satisfied, this does not guarantee the feasibility of the proposed buoyancy mechanism: we must, additionally, be sure that this condition is accomplished at a power below the critical power that can jeopardise the structural integrity of the cladding. Thus, it is important to relate the fuel  
 135 and coolant temperatures to the power being generated in the fuel. For transients in which reactivity  $\rho$  is much lower than the delayed neutron fraction  $\rho \ll \beta$ , the resulting reactor period would be considerably longer than the fuel thermal time constant  $\tau$  given by [14]:

$$\tau \approx R_f M_f c_f \quad (11)$$

where  $M_f$  and  $c_f$  are the mass and specific heat capacity of the fuel, respectively, and  $R_f$  is the fuel thermal resistance given by:

$$R_f = \frac{1}{4\pi L\kappa_f} + \frac{1}{2\pi r_g L h_g} + \frac{1}{2\pi\kappa_s L} \ln\left(\frac{r_{s2}}{r_{s1}}\right) + \frac{1}{2\pi r_{s2} L h_c} \quad (12)$$

where  $\kappa_f$  is the thermal conductivity of the fuel,  $L$  the fuel rod length,  $r_g$  and  $h_g$  are the effective gap radius and heat transfer coefficient, respectively,  $r_{s2}$  and  $r_{s1}$  the outer and inner cladding radius, respectively,  $\kappa_s$  the thermal conductivity of the cladding, and  $h_c$  the coolant heat transfer coefficient.

It should be mentioned that Eq. (12) refers to the peak fuel temperature (centerline or hollow), not to the average fuel temperature. The latter is the temperature upon which density depends. A correction could be introduced by multiplying the first term in the right-hand side of Eq. (12) by  $\frac{1}{2}$  [19]. However, the use of a peak fuel temperature, on one hand, results in an overestimation of the ballast pellet volume, but, on the other hand, in an underestimation of the power at which the buoyancy becomes effective. These effects will be somewhat compensatory, and, in view of the uncertainties in this preliminary assessment, let us use the peak fuel temperature in our calculations.

For the case where the reactor period is much longer than  $\tau$ , the fuel and coolant temperatures can be expressed as functions of the power  $P$  as [14]:

$$T_f = \left[ R_f + \frac{1}{2\dot{m}_c c_c} \right] P + T_i \quad (13)$$

and

$$T_c = \frac{1}{2\dot{m}_c c_c} P + T_i \quad (14)$$

where  $\dot{m}_c$  is the coolant mass flow rate and heat capacity, respectively; and  $T_i$  the coolant inlet temperature.

Thus, using the equations above, we find that the point at which the condition given by Eq. (10) is met occurs at a power given by:

$$P^* = \frac{\rho_{c,0} - \rho_{\text{eff},0} - T_i (\alpha_c - \alpha_{\text{eff}})}{\frac{\alpha_c - \alpha_{\text{eff}}}{2\dot{m}_c c_c} - \alpha_{\text{eff}} R_f} \quad (15)$$

To better understand the implications of these results, we assume some typical values for the relevant parameters. For the calculation of the thermal

**Table 2.** Design parameters of the HLMFR core concept considered, from [20].

Parameter	Value
Power	600 MW <sub>e</sub>
Pellet outer radius	3.3 mm
Cladding inner radius	3.4 mm
Cladding outer radius	4.55 mm
Pitch-to-diameter ratio	1.5
Length of upper plenum	100 cm
Length of lower plenum	10 cm
Active pin length	100 cm
Pin-fuel volume fraction	54.4%
Pin-steel volume fraction	45.6%
Average linear pin power	11.5 kWm <sup>-1</sup>

resistance, we take:  $\kappa_f = 2 \text{ Wm}^{-1}\text{K}^{-1}$ ,  $\kappa_s = 15 \text{ Wm}^{-1}\text{K}^{-1}$ ; from [15],  $h_g =$   
165  $5678.26 \text{ Wm}^{-2}\text{K}^{-1}$ ,  $h_c = 34069.58 \text{ Wm}^{-2}\text{K}^{-1}$ ; and, from Table 2,  $r_{s2} = 4.55$   
mm,  $r_{s1} = 3.4$  mm, with a core length of  $L = 100$  cm. These result in a  
fuel thermal resistance of  $R_f \approx 4.39 \times 10^{-2} \text{ KW}^{-1}$ . For the coolant, we take  
 $c_c = 160 \text{ JK}^{-1}\text{kg}^{-1}$ . The maximum coolant velocity allowed for lead-based  
coolants is in the range 2–3  $\text{ms}^{-1}$  because of issues of erosion [21]. Then,  
170 for the channel dimensions given in Table 2, the coolant mass flow rate is  
 $\dot{m}_c = 2 \text{ kg s}^{-1}$ .

For the average nominal linear pin power, we take a value of  $115 \text{ W cm}^{-1}$ ,  
as in Table 2 [20]. Taking an inlet temperature of  $T_i = 750 \text{ K}$ , corresponding  
with a nominal linear pin power of  $100 \text{ W cm}^{-1}$ , then results in fuel and  
175 coolant temperatures that vary as functions of linear pin power as shown in  
Fig. 5.

Fig. 6 shows how the densities of Pb-Bi eutectic and Pb coolants will  
vary as functions of linear pin power according to these equations along with  
the variation of the effective density of MOX (Fig. 6) fuels. In these figures,  
180 the choice of the fraction of tungsten ballast pellets used was more or less  
arbitrary, with the only purpose being to obtain an estimate of the amount of  
ballast needed to stop the transient safely, i.e. to ensure that fuel rod ejection  
occurs at a linear power significantly smaller than a certain design constraint,  
for example, the  $472 \text{ W cm}^{-1}$  limit suggested by Hitachi [8]. However, as will  
185 be apparent to the reader, the nuclear designer has a certain freedom of choice

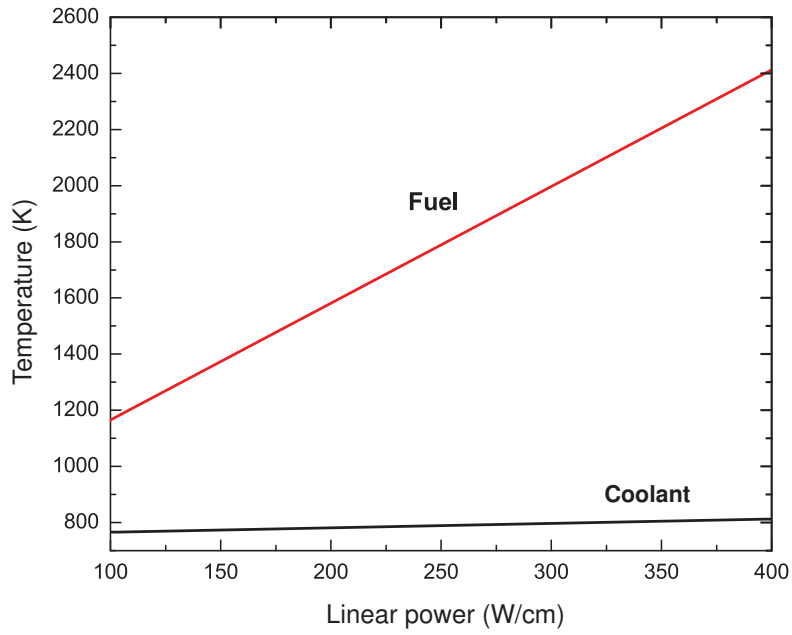


Fig. 5. Fuel and coolant temperatures as functions of linear pin power.

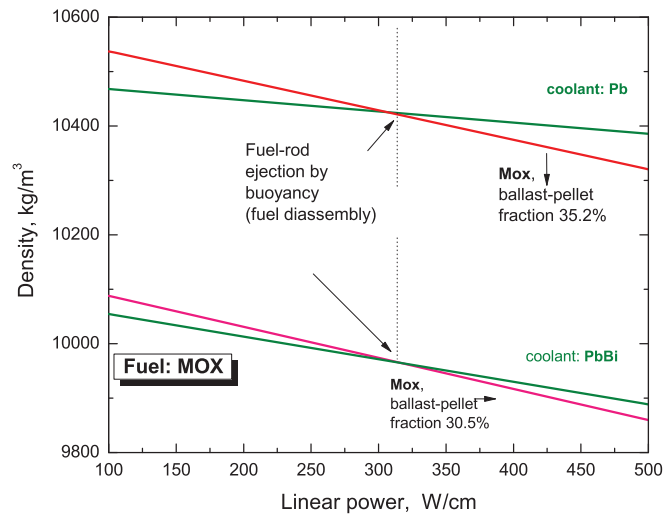


Fig. 6. Densities of coolants and MOX fuel as functions of linear pin power.

over the maximum power at which the fuel rod is ejected. If the fraction of ballast is reduced from the values used in Fig. 6, ejection will start at a lower linear power, but the system will also become more sensitive to small changes of temperature.

190 Next, we need to obtain a first estimate of the amount of negative reactivity insertion caused by the buoyancy-driven ejection of the fuel rod when the Eq. (10) condition is met. This will be our objective in the next section.

## 2.2. The negative reactivity insertion

195 In this section we will provide some first estimation on the negative reactivity insertion. This is a difficult calculation to accurately predict. Substantially uncertainties will be necessary introduced at every step of the analysis from the unavoidable idealizations required if analytical expressions are desired. If more precise calculation are desired more complex iterative methods will be required. For example, in view of several uncertainties, the simplest  
 200 lumped model for heat transfer to arrive at the buoyancy-driven parameter and the terminal velocity seems for preliminary result preferable. But as mentioned before, this is very approximate and can cause significant error in the prediction of reactivity addition rate and the time scale involved for the buoyancy-driven mechanism to control the transient. Therefore, the negative reactivity insertion reported result from idealizations and is therefore  
 205 not intended to typify negative reactivity estimates.

At the moment fuel rod ejection starts the maximum reactivity is given by

$$\rho_0 = \gamma_c \Delta T \quad (16)$$

210 where  $\gamma_c$  is the (positive) coolant temperature coefficient of reactivity and

$$\Delta T = T_c - T_c(0) \quad (17)$$

is the increase in coolant temperature from the initial value  $T_c(0)$  to the temperature  $T_c$  when ejection occurs, i.e. at power  $P = P^*$ .

The negative reactivity insertion due to the sudden upward motion of the fuel rod over a small time-step  $\Delta t$  is:

$$\Delta \rho = - \left| \frac{\partial \rho}{\partial z} \right| \left| \frac{\partial z}{\partial t} \right| \Delta t = - \left| \frac{\partial \rho}{\partial z} \right| V_t \Delta t \quad (18)$$

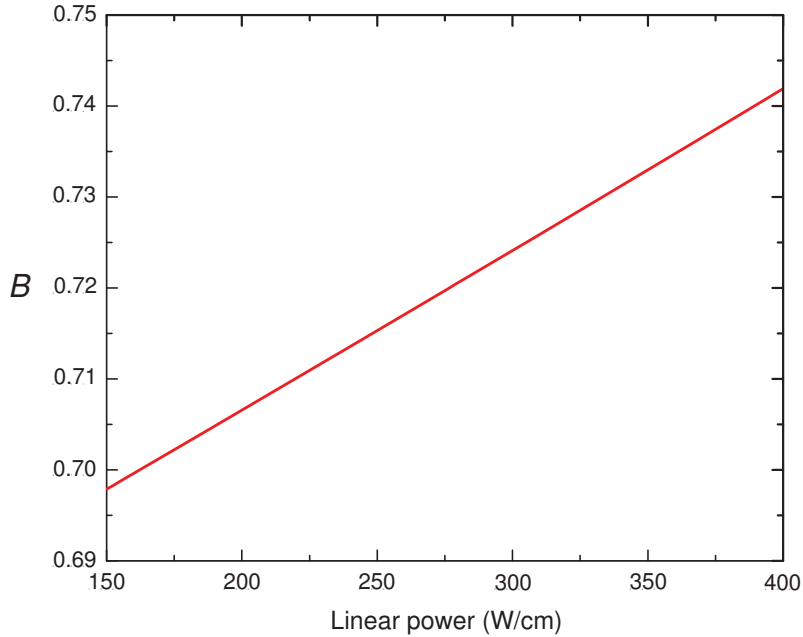


**Fig. 7.** The buoyancy-driving parameter  $B$  with lead coolant and  $\text{UO}_2$  fuel as a function of linear pin power.

215 where  $V_t$  is approximately the terminal velocity of the cylindrical fuel rod, given by [13]:

$$V_t = \sqrt{\frac{2gL}{C_d} B} \quad (19)$$

where  $g$  is the acceleration due to gravity,  $L$  is the fuel rod length,  $C_d$  is the drag coefficient, and  $B$  is a buoyancy-driving parameter defined as:

$$B = \sqrt{\frac{\rho_c - \rho_{\text{eff}}}{\rho_{\text{eff}}}} \quad (20)$$

220 Using the representative values specified in the previous section, the relationship between  $B$  and linear pin power for lead coolant and  $\text{UO}_2$  fuel is as shown in Fig. 7.

225 Now, in sufficiently slow transients, as soon as the condition given by Eq. (10) is satisfied, there will be a small prompt jump in power, but then the system will come to equilibrium as the rise in fuel and coolant temperatures and the increase in  $B$  compensate for  $\varrho_0$ , sending  $\varrho(t) \rightarrow 0$ . Thus, neglecting the effect of the negative fuel temperature coefficient of reactivity and other

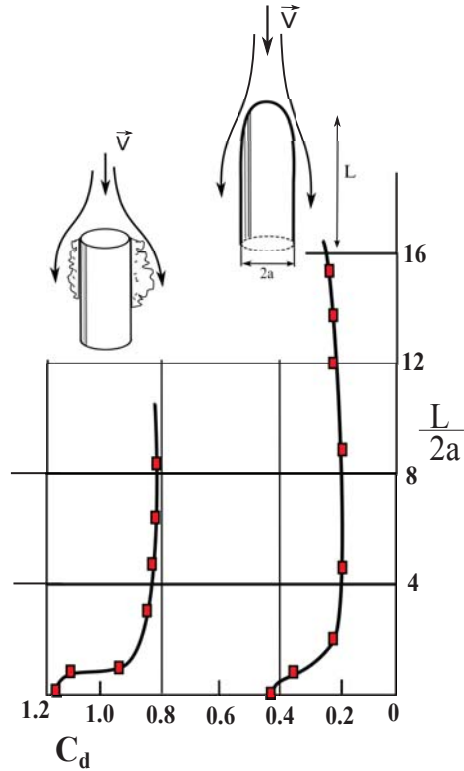


**Fig. 8.** Drag coefficients of blunt-nosed and rounded-nosed cylinders versus fineness ratio  $L/2a$  [10].

negative feedback mechanisms, the new equilibrium power will be given by [14]:

$$P(\infty) = P^* + 2\dot{m}_c c_c \left[ \frac{\varrho_o}{\gamma_c} \right] \quad (21)$$

Using the power  $P(\infty)$  we can calculate the coolant and fuel temperatures from Eqs. (13) and (14) and then their respective densities. This then allows us to find the value of the buoyancy parameter  $B$  given by Eq. (20). For example, taking  $\Delta T = \varrho_o/\gamma_c \approx 5$  K, we obtain an approximate value for  $B \approx 0.1$ . The drag coefficient  $C_d$  will be between 1.2 for a blunt-nosed cylinder or 0.2 for a rounded nose, as shown in Fig. 8 [10]. Thus, for an optimized fuel rod with a rounded end-cap, as depicted in Fig. 9, we can assume  $C_d = 0.2$ , and with a total fuel rod length (including plenums) of 210 cm (see Table 2), we obtain a terminal velocity of  $V_t \approx 1.44$  m s<sup>-1</sup>.

Finally, we need an estimate of the variation of reactivity with the dis-

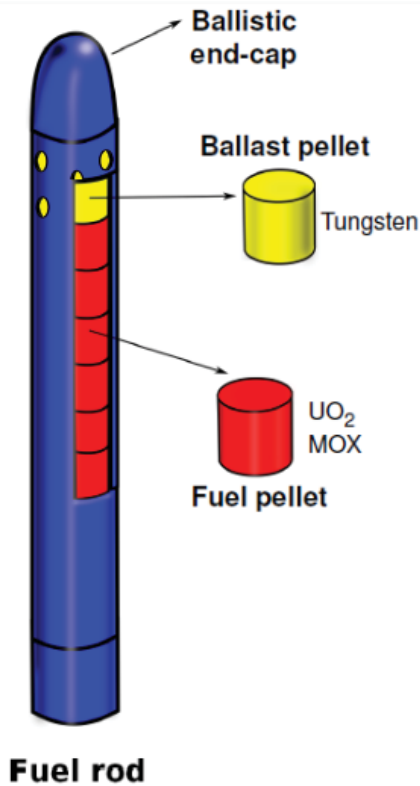


**Fig. 9.** A possible optimized fuel rod design for a lead or lead-bismuth cooled reactor. The end-cap is rounded to enhance the ejection velocity.

placement of the ejected fuel rod, i.e.  $\partial\rho/\partial z$ . Unfortunately, this is a highly  
 240 uncertain parameter; its accurate computation requires knowledge of the  
 specific location at which the fuel rod ejection occurs, as well as the spe-  
 cific design of the rod. A calculation performed using the SCALE 6 software  
 [6] for a typical fuel rod channel, using lead as the coolant and reflective  
 245 boundary conditions is translate into assuming a homogeneous core in which all  
 the elements of the core have ballast pellet and also all are moving which is  
 within the linear fuel management model in which is assumed that the total  
 core reactivity is the summation of the reactivity of each element. The use of  
 this linear model, although admittedly is rather simplified, nevertheless will  
 250 allow to provide with a conservative value of  $\partial\rho/\partial z \approx -50 \text{ pcm cm}^{-1}$ . Then  
 using our previously calculated estimate of the fuel rod terminal velocity, we  
 have a rate of negative insertion on  $-7200 \text{ pcm s}^{-1}$ . Taking a typical posi-  
 tive coolant temperature coefficient of reactivity to be  $0.36 \text{ pcm K}^{-1}$  [20] and  
 $\Delta T = 5 \text{ K}$ , the time needed for the buoyancy-driven mechanism to control  
 255 this transient will be a tiny fraction of a second once the Eq.(10) is met.

Thus, the foregoing calculations indicate that by using a modest fraction  
 ( $\sim 15\%$ ) of tungsten ballast pellets the fuel rod will be endowed with a reliable  
 self-ejection mechanism during temperature transients. It should be noted  
 that, in these preliminary calculations, other components of the fuel rod

260 which can reduce its effective density even more were neglected, the most  
important being the gas plenum chambers (if fission gases are not vented  
directly into the coolant). However, the potential reduction in the effective  
fuel rod density due to the gas plenums can be compensated by using tungsten  
rather than stainless steel for the lower and upper plenums in the fuel rod.

### 265 3. Conclusions

In this paper we explored the possibility of taking advantage of buoy-  
ancy forces in heavy liquid metal cooled fast reactors to endow the fuel rod  
with a reliable and passive negative feedback mechanism through fuel rod  
ejection (a fuel self-disassembly mechanism) during a temperature transient,  
270 compensating the positive coolant temperature coefficient of reactivity that  
some fast reactors feature. It was deduced that, through the use of tung-  
sten ballast pellets introduced into the fuel rod design, such a mechanism is  
feasible, with the volume occupied by the ballast pellets being less than 15%.

This preliminary assessment was based on unavoidable idealizations, some  
275 conservative and others non-conservative. It should not be misconstrued  
as a definitive, detailed analysis. Additional R&D is required to further  
explore the possibilities of this concept, to seek optimal values for the design  
variables, and to determine real practical applicability as details are refined.  
Only then will the feasibility of the proposed concept be fully established.

### 280 4. Appendix

#### •The use of gas plenum.

In our previous calculations, the gas plenum was not taken into account. The  
gas plenum length could be typically the same of the active length, and then  
an extra fraction of dedicated ballast would be necessary to avoid buoyancy.  
285 Because the density of the fission gas can be neglected in comparison with  
the ballast, then it is easy to see that the fraction of volume of gas plenum  
with ballast required should be  $\approx \frac{\rho_c}{\rho_w}$  where  $\rho_c$  and  $\rho_w$  are the density of  
the coolant and the ballast, respectively. Nevertheless, there is an actual  
trend to eliminate fission gas plenums and to vent fission product gases to  
290 the primary coolant system in a controlled manner,[1],[9]. Venting the fuel  
pins enables deep burnups required to sustain the core, for over 40 years and  
greatly reduces the probability of cladding failures. In addition, in lead cooled  
and even more in lead bismuth cooled reactors the use of gas plenums and  
the retention of fission gas plenums have been recently questioned,

295 **Nomenclature**

- $B$  = buoyancy parameter defined by Eq. (20)  
 $C_d$  = drag coefficient  
 $c_i$  = heat capacity of material  $i$   
 $F_f$  = volume fraction of fuel  
300  $g$  = acceleration due to gravity  
 $h$  = heat transfer coefficient  
 $L$  = length (of fuel pin or fuel rod)  
 $\dot{m}_c$  = coolant mass flow  
 $M_f$  = mass of fuel  
305  $P$  = pin power  
 $P^*$  = pin power at onset of rod ejection  
 $r$  = radius  
 $R_f$  = thermal resistance of fuel pin  
 $t$  = time  
310  $T$  = temperature  
 $T_i$  = inlet temperature of coolant  
 $V_t$  = terminal velocity  
 $z$  = vertical coordinate

315 **Greek symbols**

- $\alpha_i$  = rate of change of density of material  $i$  with temperature  
 $\beta$  = fraction of delayed neutrons  
 $\gamma_c$  = coolant temperature coefficient of reactivity  
 $\kappa_i$  = thermal conductivity of material  $i$   
320  $\rho_i$  = density of material  $i$   
 $\rho$  = reactivity

**Subscripts**

- $c$  = coolant  
325  $f$  = fuel  
 $g$  = gap  
 $s$  = stainless steel  
 $w$  = tungsten

330 **ACKNOWLEDGEMENTS**

This research was supported by the Spanish Ministry of Economy and Competitiveness under fellowship grant Ramon y Cajal: RYC-2013-13459.

## References

- 335 [1] Ahlfeld C., Burke T., Ellis T., Hejzlar P. 2011. Conceptual Design of a 500 MWe Traveling Wave Demonstration Reactor Plant. Proceedings of ICAPP 2011.Nice, France, May 2-5, 2011.Paper 11199.
- [2] Alemberti, A., 2012. The European lead fast reactor: design, safety approach and safety characteristics. In: IAEA Technical Meeting on Impact of Fukushima Event on Current and Future FR Designs, Dresden, Germany. <http://www.iaea.org/NuclearPower/Meetings/2012/2012-03-19-03-23-TM-NPTD.html>
- 340 [3] Alessandro, A., 2014. Final Report Summary - LEADER (Lead-cooled European Advanced Demonstration Reactor). European Commission Community Research and Development Information Service. <http://cordis.europa.eu/result/rcn/147643.en.html>
- 345 [4] Arias, F.J., 2014. The phenomenology of packed beds in heavy liquid metal fast reactors during postaccident heat removal: The self-removal feedback mechanism. Nucl. Sci. Eng. 178(2), 240–249.
- [5] Arias, F.J., Parks, G.T. 2015. Does it really make sense to use fission gas plenums in a lead-bismuth-cooled fast reactor?, Progress in Nuclear Energy. 85, p.p. 491-497
- 350 [6] Bowman, S.M., 2011. SCALE 6: Comprehensive nuclear safety analysis code system. Nucl. Technol. 174(2), 126–148.
- [7] Di Maio, D.V., Cretara, L., Giannetti, F., Peluso, V., Gandini, A., Manni, F., Caruso, G., 2014. An alternative solution for heavy liquid metal cooled reactors fuel assemblies. Nucl. Eng. Des. 278, 503–514.
- 355 [8] Ganda, F., Arias, F.J., Vujic, J., Greenspan, E., 2012. Self-sustaining thorium boiling water reactors. Sustainability 4, 2472–2497.
- [9] Gilleland J., Petroski R., Weaver K. 2016. The Traveling Wave Reactor: Design and Development. Engineering, 2. 8896
- 360

- [10] Hart, R.G., 1955. Flight investigation at Mach numbers from 0.8 to 1.5 to determine the effects of nose bluntness on the total drag of two fin-stabilized bodies of revolution. Technical note 3549. National Advisory Committee for Aeronautics NACA.
- 365 [11] Hejzlar, P., Driscoll, M.J. Kazimi, M.S., 2002. Conceptual Reactor Physics Design of a Lead-Bismuth-Cooled Critical Actinide Burner. Technical report MIT-ANP;TR-069. Massachusetts Institute of Technology Advanced Nuclear Power Technology Program, Cambridge, MA.
- 370 [12] Inco Databooks, 1968. Austenitic Chromium-Nickel Stainless Steels at Elevated Temperatures – Mechanical and Physical Properties (2980). Available from <http://www.nickelinstitute.org/>.
- [13] Janna, W.S., 2010. Introduction to Fluid Mechanics. Fourth Edition. CRC Press, Boca Raton, FL.
- 375 [14] Lewis, E.E., 1977. Nuclear Power Reactor Safety. John Wiley and Sons, New York, NY.
- [15] Massoud, M., 2005. Engineering Thermofluids: Thermodynamics, Fluid Mechanics, and Heat Transfer. Springer-Verlag, Berlin, Heidelberg, Germany.
- 380 [16] Nuclear Energy Agency, 2007. Handbook on Lead-bismuth Eutectic Alloy and Lead Properties, Materials Compatibility, Thermal-hydraulics and Technologies. <https://www.oecd-nea.org/science/reports/2007/nea6195-handbook.html>
- 385 [17] Popov, S.G., Carbajo, J.J., Ivanov, V.K., Yoder, G.L., 2000. Thermophysical Properties of MOX and UO<sub>2</sub> Fuels Including the Effects of irradiation. Technical report ORNL/TM-2000/351. Oak Ridge National Laboratory, Oak Ridge, TN.
- [18] Qvist, S., Greenspan, E., 2014. An autonomous reactivity control system for improved fast reactor safety. *Prog. Nucl. Energy.* 77, 32–47.
- 390 [19] Todreas, N.E., Kazimi, M.S., 2011. Nuclear Systems Volume I: Thermal Hydraulic Fundamentals. Second edition. CRC Press, Boca Raton, FL.

- [20] Tucěk, K., Carlsson, J., Wider, H., 2006. Comparison of sodium and lead-cooled fast reactors regarding reactor physics aspects, severe safety and economical issues. *Nucl. Eng. Des.* 236, 1589–1598.
- [21] Zhang, J., Li, N., 2008. Review of the studies on fundamental issues in LBE corrosion. *J. Nucl. Mater.* 373 (1–3), 351–377.

395